# Carotenoid $S_1$ State in a Recombinant Light-Harvesting Complex of Photosystem II†

Tomáš Polívka,* Donatas Zigmantas, and Villy Sundström*

*Department of Chemical Physics, Lund University, Box 124, S-22100 Lund, Sweden*

Elena Formaggio, Gianfelice Cinque, and Roberto Bassi

*Facoltà di Scienze, Università di Verona, Strada Le Grazie 15, I-37134 Verona, Italy*

*Received July 31, 2001; Revised Manuscript Received October 30, 2001*

ABSTRACT: The carotenoid species lutein, violaxanthin, and zeaxanthin are crucial in the xanthophyll-dependent nonphotochemical quenching occurring in photosynthetic systems of higher plants, since they are involved in dissipation of excess energy and thus protect the photosynthetic machinery from irreversible inhibition. Nonetheless, important properties of the xanthophyll cycle carotenoids, such as the energy of their $S_1$ electronic states, are difficult to study and were only recently determined in organic solvents [Polívka, T. (1999) *Proc. Natl. Acad. Sci. U.S.A. 96*, 4914. Frank, H. A. (2000) *Biochemistry 39*, 2831]. In the present study, we have determined the $S_1$ energies of three carotenoid species, violaxanthin, lutein, and zeaxanthin, in their LHCII (peripheral light-harvesting complex of photosystem II) protein environment by constructing recombinant Lhcb1 (Lhc = light-harvesting complex) proteins containing single carotenoid species. Within experimental error the $S_1$ energy is the same for all three carotenoids in the monomeric LHCII, 13900 ± 300 $cm^{-1}$ (720 ± 15 nm), thus well below the $Q_y$ transitions of chlorophylls. In addition, we have found that, although the $S_1$ lifetimes of violaxanthin, lutein, and zeaxanthin differ substantially in solution, when incorporated into the LHCII protein, their $S_1$ states have in fact the same lifetime of about 11 ps. Despite the similar spectroscopic properties of the carotenoids bound to the LHCII, we observed a maximal fluorescence quenching when zeaxanthin was present in the LHCII complex. On the basis of these observations, we suggest that, rather than different photochemical properties of individual carotenoid species, changes in the protein conformation induced by binding of carotenoids with distinct molecular structures are involved in the quenching phenomena associated with Lhc proteins.

In higher plants, sunlight energy is collected by chlorophylls (Chl's[1]) and carotenoids bound to light-harvesting complexes (Lhc's). One of the most abundant pigment−protein complexes with an antenna function is LHCII, which contains Chl-a, Chl-b, and a variety of carotenoids for light absorption and photoprotection (*1*). More than half of the light used for photosynthesis is harvested by the chromophores of this protein complex, which is located on the periphery of photosystem II. The LHCII protein serves as a primary donor of excitation energy, which is then transferred to the reaction center, where charge separation occurs. In addition to the light-harvesting function, carotenoids are known to effectively quench the chlorophyll triplet states (*2*), to scavenge singlet oxygen (*3*), and to play an essential role in down-regulating energy flow by dissipation of excess energy in antennae (*4*). In this photoprotection function, carotenoids participate in regulating the amount of light energy used for driving photochemical reactions in the reaction center according to the given light conditions by means of the xanthophyll cycle, involving three carotenoid species: zeaxanthin, antheraxanthin, and violaxanthin (*4*).

The crystal structure of the LHCII protein, determined with 3.4 Å resolution (*5*), reveals that the native form of the LHCII protein has a trimeric structure consisting of subunits of Lhcb1, -2, or -3 gene products, each of which binds seven Chl-a molecules, five Chl-b molecules, and three (or four; see below) different types of carotenoids in stoichiometric amounts of 1.8 Lut, 1 Neo, and approximately 0.2 Vio (*6*, *7*). In the crystal structure, only two central carotenoid-binding sites, called L1 and L2, are resolved. These two sites are predominantly occupied by Lut, but it was recently shown that site L2 also binds Vio though with a Lut:Vio affinity of 80:20 (*3*). Further biochemical analysis revealed two additional carotenoid-binding sites present in the LHCII protein (*8*, *9*): the N1 site, specific for Neo, and site V1, which has low affinity and has been poorly characterized so far. This violaxanthin-selective site is easily removed during detergent

† The work at Lund University was supported by the Swedish National Research Council. The work of E.F. at Lund University was supported by a travel grant from the European Community (HPRI-CT-1999-00041). Financial support to R.B. was provided by the "Target project on biotechnology" of the National Research Council (CNR) and by MURST-COFIN 2000 of Italy.

* To whom correspondence should be addressed. (T.P.) E-mail: tomas.polivka@chemphys.lu.se. Phone: +46-46-2224700. Fax: +46-46-2224119. (V.S.) E-mail: villy.sundstrom@chemphys.lu.se. Phone: +46-46-22246902. Fax: +46-46-224119.

[1] Abbreviations: BBO, β-barium borate; Chl, chlorophyll; DM, dodecyl β-D-maltoside; ESA, excited-state absorption; fwhm, full width at half- maximum; HPLC, high-performance liquid chromatography; Lhc, light-harvesting complex; LHCII, peripheral light-harvesting complex of photosystem II; LHCII-Lut, recombinant monomeric LHCII containing only lutein; LHCII-Vio, recombinant monomeric LHCII containing only violaxanthin; LHCII-Zea, recombinant monomeric LHCII containing only zeaxanthin; Lut, lutein; Neo, neoxanthin; OD, optical density; OPO, optical parametric oscillator; Vio, violaxanthin; Zea, zeaxanthin.

10.1021/bi011589x CCC: $22.00 
Published on Web 12/15/2001

treatment and seems to be occupied preferentially in plants grown under high-light conditions (*8*, *9*).

The energy-transfer processes within the LHCII complex have been the subject of many studies during the past few years. While the energy transfer between Chl-b and Chl-a is now established to occur on a time scale shorter than 6 ps (*10*−*12*), the energy-transfer pathways involving carotenoid molecules are much less understood. This situation is partially due to the unique photophysical properties of carotenoids, which are determined by the conjugated $\pi$-electron backbone of their polyene chain. Because the conjugated chain has $C_{2h}$ symmetry, a transition between ground $S_0$ and $S_2$ states is optically allowed, resulting in a strong absorption in the spectral region 420−550 nm. In contrast, the $S_0-S_1$ transition is optically forbidden, because the $S_1$ state has the same symmetry as the ground state (*13*). By fundamental laws of photophysics, after being excited to the $S_2$ state, a carotenoid molecule will relax on the subpicosecond time scale to the $S_1$ state (*14*), the lifetime of which is determined by conjugation length and varies between 3 and 30 ps for carotenoids occurring in nature (*15*). In the case of LHCII and related light-harvesting complexes, the situation is further complicated by the spectrally overlapping carotenoid $S_0-S_2$ and chlorophyll Soret transitions. This fact, together with ultrafast dynamics of the carotenoid $S_2$ state and inability to directly locate the $S_1$ energy, makes any detailed studies of energy transfer between carotenoids and chlorophylls rather difficult. Nevertheless, in a few studies it was proven that a significant part (~80%) of carotenoid−Chl energy transfer utilizes the $S_2-Q_x$ pathway with transfer rates corresponding to less than 100 fs (*16*, *17*). Very recently, it was also suggested that in the case of Chl-b even the higher $B_x$ state can be an acceptor of energy transferred from the $S_2$ state of carotenoids (*18*). Nevertheless, the exact assignment of the donors and acceptors involved in this ultrafast transfer process is still a subject of debate.

Despite increasingly better understanding of both carotenoid $S_2$−Chl and Chl−Chl energy transfer in Lhc complexes, also supported by the knowledge of structural information, the role of the carotenoid $S_1$ state in energy-transfer and/or energy-dissipation processes remains essentially unknown. As far as carotenoid−Chl energy transfer is concerned, recent time-resolved experiments on trimeric LHCII complexes at 77 K (*17*) by Gradinaru et al. revealed a 1 ps component, which was ascribed to the carotenoid $S_1$−Chl energy transfer. Using two-photon excitation, Walla et al. attributed a 200 fs rise time of the Chl-a excited state to carotenoid $S_1$−Chl energy transfer (*19*). On the other hand, Croce et al. did not find any evidence for the carotenoid $S_1$−Chl pathway using recombinant LHCII complexes (*18*).

Besides the light-harvesting processes, the $S_1$ state of carotenoid is believed to play a role in the energy dissipation. One of the suggested mechanisms, involving direct photophysical quenching, is the so-called "molecular gear shift" (*20*). This process assumes that the carotenoid zeaxanthin (11 conjugated C═C bonds), which under high-light conditions is created in the xanthophyll cycle by deepoxidation of Vio (9 C═C bonds), has its $S_1$ level below the $Q_y$ transition of Chl-a and thus protects chlorophylls by accepting and dissipating excess energy. On the other hand, under low-light conditions Zea is epoxidated back to Vio, which is assumed to have an $S_1$ level above the Chl-a $Q_y$ due to a shorter conjugation length, rather allowing energy transfer from the carotenoid $S_1$ state to Chl-a. However, this mechanism was challenged by direct measurements of the $S_1$ energies of both carotenoids in solution by means of near-infrared transient absorption spectroscopy (*21*) and fluorescence (*22*), showing that the $S_1$ levels of both carotenoids in solution are lower than the $Q_y$ transition of Chl-a. Although this result excluded the $S_1$ to $Q_y$ transfer from Vio, a direct quenching of the $Q_y$ state of Chl-a by the $S_1$ state of Zea cannot be ruled out, especially because it was found that fluorescence quenching is enhanced in antenna complexes enriched with Zea (*23*−*25*). Thus, to obtain more knowledge about the role of the carotenoid $S_1$ level in the quenching mechanisms, information about the carotenoid $S_1$ energies in the LHCII protein is necessary.

Recently, we developed an experimental approach based on femtosecond spectroscopy to determine the $S_1$ energies of carotenoids by scanning the $S_1-S_2$ excited-state absorption in the near-infrared region (*21*, *26*), which constitutes a powerful alternative to spectroscopic techniques also used to determine the carotenoid $S_1$ energies by detection of the weak $S_1$ fluorescence (*22*, *27*) or by resonance Raman spectroscopy (*28*). Contrary to the fluorescence and resonance Raman methods, the near-infrared femtosecond technique is not restricted to measurements of carotenoids in solution and can also be used for chromophores in their natural protein environment. Another experimental approach based on two-photon excitation was already used to determine the energy of the carotenoid $S_1$ energy in native LHCII complexes (*19*).

One of the main problems when Lhc complexes are studied is the presence of a few different carotenoids, the absorption spectra of which overlap and thus prevent a selective excitation of only one carotenoid species. The use of recombinant LHCII proteins can overcome this problem since the Lhc protein was overexpressed in bacteria and then in vitro refolded with a single carotenoid species (*3*). The success of this approach relies on the fact that the recombinant pigment protein complex has been proven to maintain the functional characteristics of the native LHCII.

In this work we study spectroscopic properties of the carotenoid $S_1$ state and its role in the light-harvesting and energy-dissipation processes in the recombinant monomeric LHCII complexes containing only Lut, Vio, or Zea by means of femtosecond time-resolved spectroscopy applied in the broad spectral range extending from 500 to 1800 nm.

## MATERIALS AND METHODS

*Preparation of the Recombinant LHCII Complexes*. The DNA construct for LHCII overexpression was obtained by mutagenesis of the cDNA Lhcb1 clone (*29*). A sequence encoding six histidine tails was inserted at the 3′ end before the stop codon. The resulting fragment was inserted into the pQE52 Qiagen expression vector (pDS series) (*30*). The LHCII apoprotein was isolated from the SG13009 strain transformed with the LHCII construct as previously described (*31*) with modifications according to Croce et al. (*3*). Purification of refolded holocomplexes was achieved by a $Ni^{2+}$ chelating column (Pharmacia Source 15S) followed by ion-exchange chromatography and by ultracentrifugation in glycerol gradient (15−40% including 0.06% DM and 10 mM Hepes, pH 7.6; 12 h at 60000 rpm in a SW60 Beckman

rotor). HPLC analysis of acetone-extracted pigments was according to Gilmore (*32*). Before the experiments, the purified samples were stored in the dark at −55 °C.

*Steady-State Spectroscopy*. Absorption spectra were recorded at room temperature with an Aminco DW-2000 spectrophotometer in a cuvette with a 1 cm path length using buffer containing 5 mM Hepes and 0.06% DM at pH 7.6. The Soret region of the absorption spectra was fitted as a sum of single-pigment spectra, taking into account the relative stoichiometry of the pigments.

*Time-Resolved Spectroscopy*. The monomeric LHCII complexes were dissolved in a buffer (10 mM Hepes/NaOH, pH 7.6, 0.03% DM), with $H_2O$ replaced by $D_2O$ to allow measurements above 1300 nm, where $H_2O$ has a strong absorption. It was checked that such a change does not affect the absorption spectra of the LHCII complexes. Samples having OD values of 0.8−0.9/mm at 680 nm and 0.15−0.2/mm at 510 nm were used to allow excitation at the latter wavelength. All measurements were carried out at 4 °C with the sample in a 1 mm path length glass cuvette placed in a specially designed cooling chamber, enabling precise adjustment of temperature. For the fluorescence single-photon-counting measurements, all studied samples were dissolved in the same buffer to achieve an OD of less than 0.01/mm at 680 nm. The single-photon-counting measurements were carried out at room temperature in a 1 cm path length quartz cuvette.

The femtosecond spectrometer used in these studies is based on an amplified Ti:sapphire laser system, with tunable pulses obtained from two optical parametric amplifiers and/or white-light continuum generation. Femtosecond pulses obtained from the Ti:sapphire oscillator operating at a repetition rate of 82 MHz were amplified by a regenerative Ti:sapphire amplifier pumped by a Nd:YLF laser operating at a repetition rate of 5 kHz and producing ∼120 fs pulses with an average output power of ∼1 W and a central wavelength of 800 nm. For measurements in the near−infrared region, the amplifier output was divided by a 75/25 beam-splitter to pump two independent parametric amplifiers for generation of the pump and probe pulses. The wavelength of the pump pulses was fixed to either 510 or 650 nm, while the parametric amplifier used for generation of probe pulses was controlled by a computer, enabling direct scanning of the wavelength of the probe pulses over the spectral region 850−1800 nm. For measurements in the visible range, one part of the amplifier output was used to pump an optical parametric amplifier for generation of the 510 nm pump pulses, while the other was used to produce white-light continuum probe pulses in a 1 cm sapphire plate. In all measurements, the mutual polarization of the pump and probe beams was set to the magic angle (54.7°) using a polarization rotator placed in the pump beam path. The instrument response function was measured by frequency mixing the pump and probe pulses in a $LiIO_3$ crystal; the obtained cross-correlation was fitted to a Gaussian function with a fwhm of 170−200 fs for measurements with the two optical parametric amplifiers (the actual fwhm depends slightly on the wavelength of the probing pulses) or 120−140 fs when the white-light continuum was used for probing.

A detection system based on a three-diode arrangement in combination with a single-grating monochromator provided a spectral resolution better than 40 $cm^{-1}$. To prevent any photochemical damage of the sample during measurement, the cooling chamber with the 1 mm glass cuvette containing the sample was moved during the course of measurement, and the excitation pulses were attenuated using neutral density filters to typical energies of 100 nJ/pulse. Furthermore, absorption spectra were measured before and after the measurements to ensure that no permanent photochemical changes occurred over the duration of the experiment.

*Time-Correlated Single-Photon-Counting Measurements*. Excitation pulses were obtained by frequency doubling a synchronously pumped OPO output with a 3 mm BBO nonlinear crystal. The OPO was pumped by a Ti:sapphire femtosecond oscillator operating at a 81 MHz repetition rate, producing 80 fs pulses centered at 775 nm. The high repetition rate of the OPO output was reduced to 400 kHz by a Bragg cell pulse-picker. The excitation pulses at 650 nm had a duration of ∼150 fs and an excitation density of ∼3 nJ $pulse^{-1}$ $cm^{-2}$ at the sample place. Fluorescence was collected in a 90° geometry, and a microchannel plate photomultiplier together with conventional electronics was used to obtain the time-resolved fluorescence data. The fwhm of the response function was 80 ps. A minimum of 14000 counts were collected in the peak channel to achieve a good signal-to-noise ratio.

## RESULTS

In vitro reconstitution of maize Lhcb1 in the presence of a pigment extract from thylakoid membranes yields monomeric chlorophyll proteins with spectral properties and pigment composition identical to those obtained from the protein purified from maize thylakoids (*3*). Accordingly, we found that the LHCII control sample binds 1.8 Lut, 0.2 Vio, and 1.0 Neo per polypeptide on the basis of 12 Chl molecules per polypeptide (*3*, *5*, *6*). When Lut, Vio, or Zea was used as the only carotenoid species in the reconstitution mixture, only two carotenoids per polypeptide were bound in agreement with previous results showing that these carotenoids can bind to both sites L1 and L2 but not to site N1 (*3*).

Steady-state absorption spectra of all studied samples normalized to the Soret band of Chl-b are shown in Figure 1. Absorption bands are ascribed to the absorption of Chl-a ($Q_y$ transition around 674 nm, Soret band at 440 nm) and Chl-b ($Q_y$ transition at 650 nm, Soret band centered at 475 nm). The broad feature between 550 and 630 nm is due to contributions from the $Q_x$ transitions and higher vibrational $Q_y$ transitions of both Chl-a and Chl-b. Both the Soret and $Q_y$ regions of the chlorophyll absorption reflect different Chl-a/Chl-b ratios in the reconstituted LHCII complexes, which contain eight Chl-a molecules and four Chl-b molecules (LHCII-Vio), seven Chl-a molecules and five Chl-b molecules (LHCII-Zea and LHCII-control), or six Chl-a molecules and six Chl-b molecules (LHCII-Lut). In Figure 1, the magnification of the 460−520 nm region, where the lowest allowed $S_0-S_2$ transition of the carotenoids is expected, enhances the differences among the recombinant LHCII complexes. The absorption spectrum of LHCII-Vio exhibits a pronounced shoulder at 490 nm, while the LHCII-Zea sample has a similar, but weaker, band shifted to lower energies located at around 500 nm. LHCII-Lut shows rather structureless absorption in this spectral region, with a hint

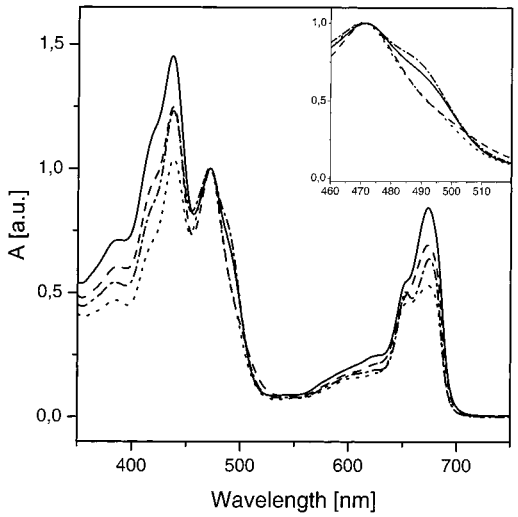


FIGURE 1: Absorption spectra of the monomeric LHCII complexes reconstituted with a single carotenoid species together with the monomeric LHCII-control complex: LHCII-Vio (solid line), LHCII-Zea (dashed line), LHCII-Lut (dotted line), and LHCII-control (dashed−dotted line). The inset shows the spectral region of carotenoid absorption. All spectra are normalized to the Chl-b Soret peak at 475 nm.

of a shoulder centered at 495 nm. Detailed fitting of this spectral region (see below) shows that this effect is a result of different spectral properties of the two luteins bound to the L1 and L2 sites. This observation is in accord with recent studies of LHCII complexes showing that the absorption spectra of the two luteins occupying the L1 and L2 sites are not identical (*18*). A shift of the carotenoid absorption band toward lower energies in the order Vio−Lut−Zea (inset of Figure 1) is a result of the change of the conjugation length of these carotenoids, increasing from 9 (Vio) to 11 (Zea) C═C bonds. A similar, more pronounced, shift is observed also for carotenoids in solution (*21*), but in the LHCII protein the absorption bands of all carotenoids are shifted to lower energies as a result of interactions with the protein environment. For comparison, the absorption spectrum of the LHCII-control sample is shown, exhibiting a shoulder centered at 490 nm as a combination of absorption of Lut, Vio, and Neo, which are all present in the native LHCII complexes with a ratio of about 1:0.11:0.55 (*3*).

Deconvolution of the Soret region into elementary spectral forms was performed as described previously (*33*, *34*), and the results are shown in Figure 2. To satisfactorily fit the spectra of LHCII-Lut, two absorption forms of this carotenoid having their $S_2$ 0−0 energies at 20250 $cm^{-1}$ (494 nm) and 20050 $cm^{-1}$ (499 nm) were needed, in agreement with previous findings that Lut has different absorption spectra when bound to the L1 and L2 sites (*18*, *33*). The Soret region of both LHCII-Vio and LHCII-Zea can be successfully fitted with only one spectral form of the carotenoid, resulting in the $S_2$ 0−0 energies of LHCII-Vio at 20200 $cm^{-1}$ (495 nm) and at 20050 $cm^{-1}$ (499 nm) for LHCII-Zea. The deconvolution of the LHCII-control absorption spectrum yielded carotenoid $S_2$ 0−0 energies peaking at 20450 $cm^{-1}$ (489 nm) and 20200 $cm^{-1}$ (495 nm) for Lut, as well as at 20320 $cm^{-1}$ (492 nm) for Vio and at 20500 $cm^{-1}$ (488 nm) for Neo, as reported previously (*33*). The error given by the fitting procedure is approximately ±100 $cm^{-1}$ in all cases. These results are consistent with the fact that site L1 is occupied only by Lut, while Vio and Lut both compete to occupy site L2.

Transient absorption spectra measured in the visible region are shown in Figure 3. To distinguish between carotenoid and chlorophyll contributions, the transient spectra were measured with two different excitation wavelengths, 510 nm corresponding to the red tail of the carotenoid $S_2$ absorption and 650 nm corresponding to the absorption of Chl-b. This allows separation of carotenoid and chlorophyll signals since at 510 nm more than 90% of the absorption is due to carotenoids (*18*). All spectra, taken 6 ps after excitation, were normalized to the maximum of the Chl-a bleaching centered at 685 nm. The transient spectra excited at 650 nm are dominated by a sharp bleaching signal originating from Chl-a. A hint of a negative feature at 655 nm is due to Chl-b bleaching, but as Chl-b to Chl-a energy transfer is almost completed within 6 ps, this feature is weak. A broad structureless signal between 520 and 640 nm is due to the combination of the $Q_x$ bleaching and weak excited-state absorption of both Chl-a and Chl-b. When excited at 650 nm, the transient absorption spectra in the visible region do not show any significant difference among the four studied samples.

Contrary to the 650 nm excitation, the transient spectra measured after 510 nm excitation (Figure 3b) show distinct spectral bands located between 500 and 600 nm in addition to the Chl-a and Chl-b bleaching bands. ESA in this spectral region is characteristic of the $S_1-S_N$ transition of carotenoids (*20*), and the LHCII complexes reconstituted with a single carotenoid have maxima located at 565 nm (LHCII-Zea), 550 nm (LHCII-Lut), and 540 nm (LHCII-Vio). All three reconstituted LHCII complexes exhibit an amplitude ratio of the carotenoid $S_1-S_N$ signals and Chl-a bleaching signal of 0.3−0.5, showing that a substantial fraction of the carotenoid $S_2$ population reaches the $S_1$ level. In the case of the LHCII-control sample this ratio drops to ∼0.1. This suggests, under the assumption that the ratio between the oscillator strengths of the carotenoid $S_1-S_N$ transition and the Chl-a $Q_y$ transition is the same for all samples, that the $S_2-Q_x$ energy-transfer pathway is more efficient in the native LHCII complex.

A direct comparison of the $S_1-S_N$ bands of the reconstituted LHCII complexes with the transient absorption spectra of the carotenoids in solution is shown in Figure 4. The shapes of the ESA bands of both LHCII-Vio and LHCII-Zea resemble closely the $S_1-S_N$ spectra observed for those carotenoids in methanol solution. In the case of the LHCII-Lut sample, the $S_1-S_N$ band is markedly broader than that observed for lutein in solution, rather consisting of two overlapping bands centered at 537 and 553 nm, suggesting the presence of two different lutein spectra due to a different interaction with the protein environment at the L1 and L2 sites. This observation again supports the results of the deconvolution of the Soret band shown in Figure 2. A comparison of the spectral position of the ESA bands shows that in the LHCII complexes they are shifted to lower energies with respect to methanol solution as a result of the interaction with the protein medium. The shift of the $S_1-S_N$ transition is different for the four studied LHCII complexes. For the LHCII-Vio sample, a shift of 900 $cm^{-1}$ (24 nm) is displayed, while the LHCII-Zea complex exhibits a significantly smaller shift of 400 $cm^{-1}$ (12 nm). For the LHCII-Lut complex, the shifts of the two bands observed in the

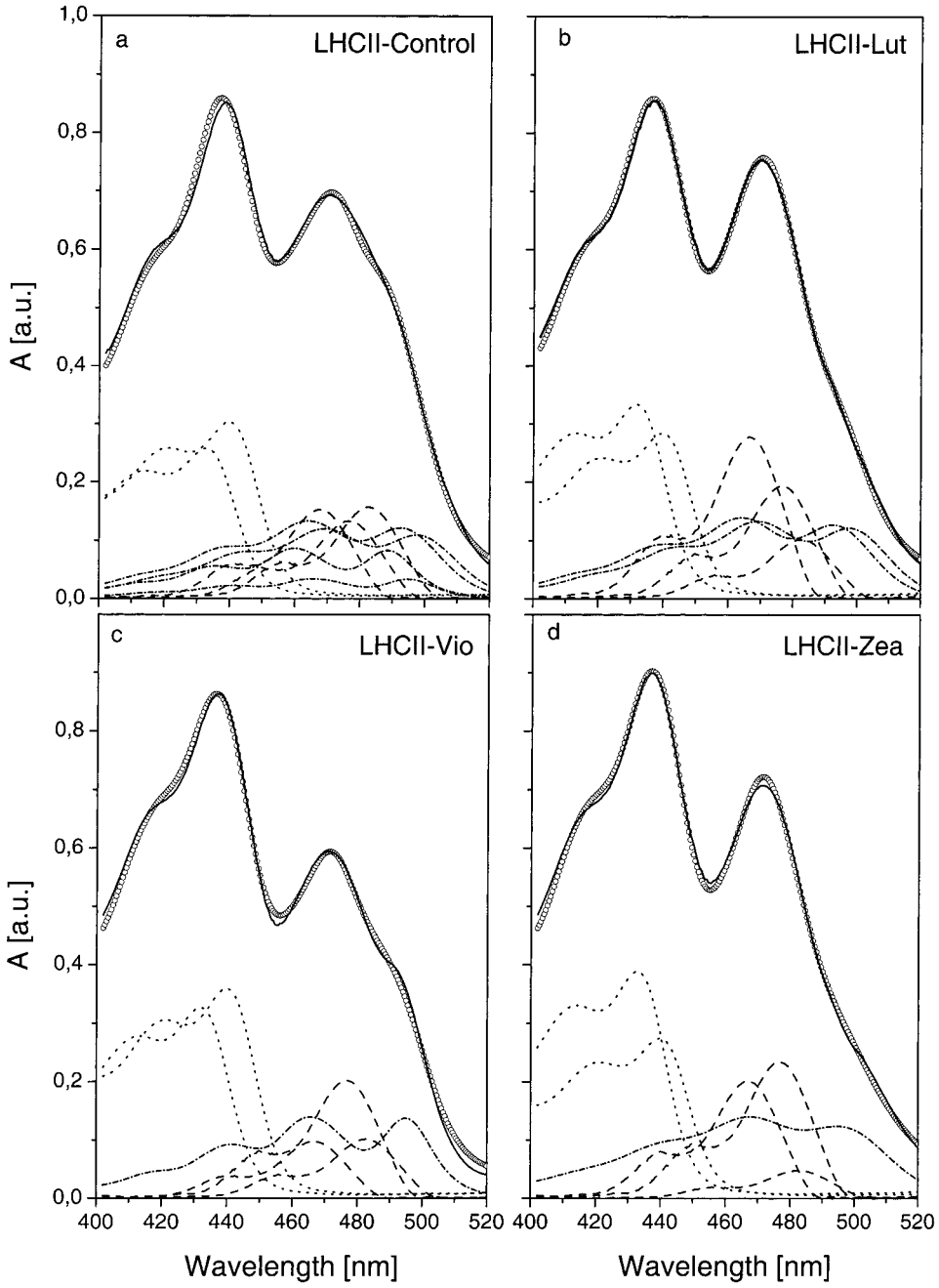


FIGURE 2: Absorption spectra and their deconvolution into spectral forms of individual pigments in the spectral region of chlorophyll Soret bands and carotenoid $S_2$ absorption. The absorption spectra of the LHCII complexes (open circles) are compared with the absorption spectra constructed as a sum (solid lines) of absorption spectra of individual pigments: Chl-a (dotted lines), Chl-b (dashed lines), and carotenoids (dashed−dotted lines).

$S_1-S_N$ spectrum are 400 $cm^{-1}$ (12 nm) and 950 $cm^{-1}$ (26 nm), respectively, suggesting that there is a much stronger protein−carotenoid interaction in one of the L sites. The LHCII-control complex in Figure 3 is compared with the $S_1-S_N$ spectrum of Lut, since this carotenoid is the most abundant in the native LHCII complex. The peak of the $S_1-S_N$ spectrum is located at 542 nm and is due to the overlapping spectra of the Lut and Vio, sitting in site L2, as well as Neo occupying the N1 site in the control sample. The $S_1-S_N$ spectrum of Neo is very similar to that of Vio (*35*). A low-energy shoulder at 558 nm is most likely due to Lut occupying site L1, since the shift from the solvent spectrum is 1000 $cm^{-1}$ (30 nm), similar to that observed in the LHCII-Lut sample. The Lut sitting in site L2 has a presumably smaller shift and thus overlap with contributions from Vio and Neo. This again suggests that markedly different interactions at the L1 and L2 sites are indeed characteristic of Lut.

To explore the carotenoid dynamics in more detail, absorption kinetics were measured at various probing wavelengths spanning the transient absorption spectrum. Kinetics probed at the maximum of Chl-a bleaching (680 nm) with excitation at 510 nm are shown in Figure 5; all studied LHCII complexes exhibit dynamics typical for Chl-b to Chl-a transfer observed elsewhere (*1*, *10*, *12*). The kinetics can be fitted by two rise components with time constants of 200−300 fs and 2−2.7 ps depending on the sample (see Table 1). The former subpicosecond component certainly includes also fast

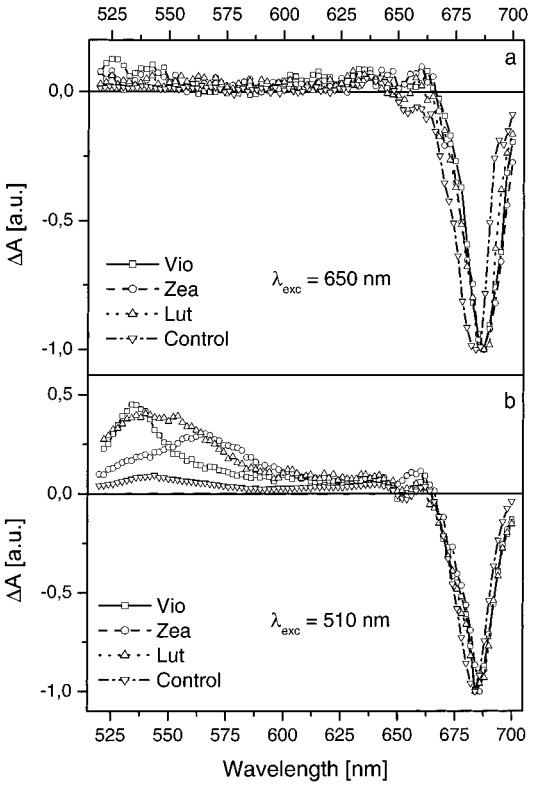


FIGURE 3: Transient absorption spectra of the LHCII complexes taken 6 ps after excitation of the Chl-b $Q_y$ band at 650 nm (a) and of the lowest energy transition of carotenoids at 510 nm (b). The spectra are normalized to the maximum of Chl-a bleaching at 685 nm.

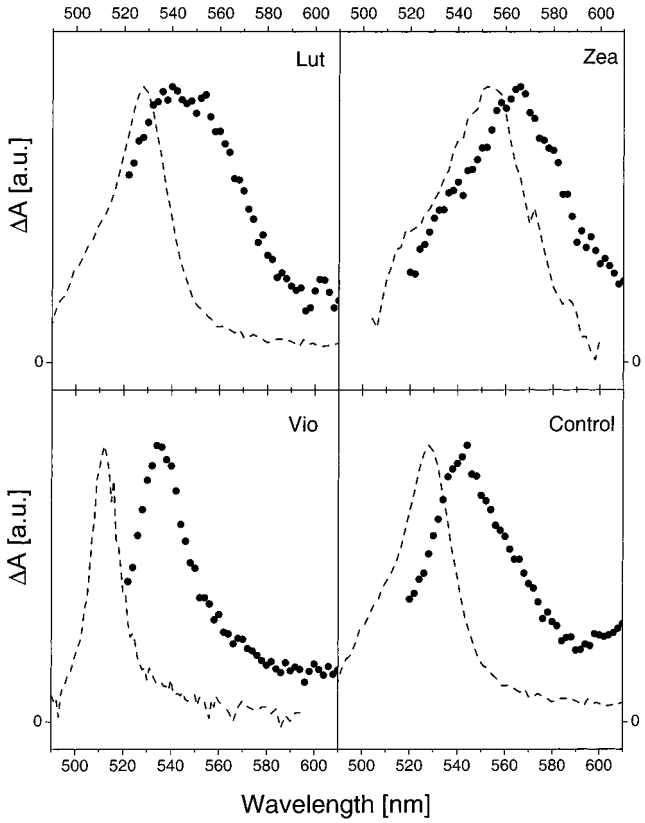


FIGURE 4: Transient absorption spectra of the LHCII complexes (circles) and corresponding carotenoids in methanol solution (dashed lines). The transient absorption spectra of the LHCII complexes were taken 6 ps after excitation at 510 nm; the transient spectra of individual carotenoids in solution were recorded 3 ps after excitation into the lowest vibrational band of the $S_0-S_2$ transition at 480 nm (Vio) and 490 nm (Lut, Zea). All transient spectra are normalized to the maximum.

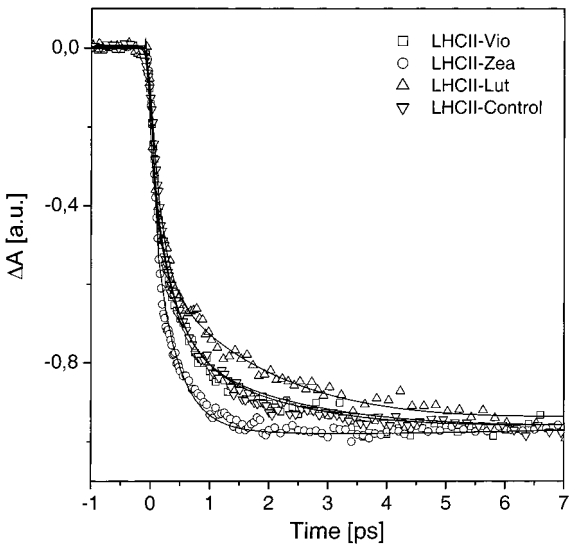


FIGURE 5: Kinetics of the Chl-a rise of the LHCII complexes detected at 680 nm following excitation of the carotenoids at 510 nm. All kinetics are normalized to the bleaching maximum. The solid lines correspond to multiexponential fits of the kinetics.

energy transfer from the carotenoid $S_2$ state to the $Q_x$ state of Chl-a, which was proven to occur on time scales faster than 100 fs (*16*−*18*), thus beyond the time resolution of our experiments. Amplitudes of the two rise times vary with the samples, most likely because of a variation of both the Chl-a/Chl-b ratio and $S_2-Q_x$ energy-transfer efficiency in the different LHCII complexes. Kinetics measured on a longer time scale (not shown) exhibit decay of the bleaching signal characterized by a time constant of about 70 ps. Such long-time dynamics was already observed in previous studies and is probably due to the equilibration among Chl-a molecules over longer distances, e.g., between different LHCII monomers (*10*, *12*). The rest (∼50%) of the decay corresponds to the 3 ns lifetime of Chl-a molecules. The 680 nm kinetics were measured for a few different excitation intensities to ensure that exciton annihilation does not affect the decays: varying the intensity by an order of magnitude caused no alterations of the kinetics. Since the kinetics probed at 680 nm are dominated by Chl-b to Chl-a dynamics, the extracted time constants (except for the subpicosecond component, which is significantly affected by contribution from $S_2-Q_x$ transfer) were then used as a guide for the fitting of the kinetics in the carotenoid region, where some contributions from chlorophyll signals are also expected.

In the region of the $S_1-S_N$ transition of carotenoids, the kinetics were measured at the maxima of the $S_1-S_N$ bands for both 510 and 650 nm excitation (Figure 6). The intensity of excitation was set to produce the same amplitude of Chl-a bleaching at 680 nm for both excitation wavelengths. For kinetics excited at 510 nm, the dominating decay with an amplitude >60% is characterized by a time constant of about 11 ps for all studied samples. In addition, the kinetic components with time constants of ∼2 ps, 70 ps and 3 ns characterizing the Chl-a dynamics were necessary to achieve satisfactory fits. The 11 ps main decay component observed in all three samples upon carotenoid excitation is then clearly

Table 1: Time Constants Extracted from Multiexponential Fits of Kinetics Measured at Various Probing Wavelengths[a]

| sample | $\lambda_{exc}$ (nm) | $\lambda_{probe}$ (nm) | $T_0$ (ps) | $A_0$ (%) | $T_1$ (ps) | $A_1$ (%) | $T_2$ (ps) | $A_2$ (%) | $A_3$ (70 ps) (%) | $A_4$ (3 ns) (%) |
|---|---|---|---|---|---|---|---|---|---|---|
| LHCII-Zea | 510 | 565 | 0.2 | −85 | 1.9 | 18 | 11 | 70 | 7 | 5 |
| | 510 | 680 | 0.2 | −73 | 2.1 | −13 | | | 47 | 53 |
| | 510 | 1600 | 0.2 | 40 | 1.6 | 3 | 10 | 36 | 7 | 12 |
| | 650 | 565 | <0.15 | −100 | 1.8 | 25 | | | 37 | 38 |
| LHCII-Vio | 510 | 540 | 0.2 | −70 | 1.9 | 20 | 10.5 | 62 | 14 | 4 |
| | 510 | 680 | 0.3 | −40 | 2.5 | −26 | | | 55 | 45 |
| | 510 | 1600 | 0.2 | 20 | 1.8 | 12 | 11 | 35 | 23 | 10 |
| | 650 | 540 | <0.15 | −100 | 1.9 | 14 | | | 60 | 26 |
| LHCII-Lut | 510 | 550 | 0.15 | −90 | 1.7 | 19 | 11.5 | 62 | 11 | 8 |
| | 510 | 680 | 0.2 | −35 | 2.7 | −42 | | | 60 | 40 |
| | 510 | 1600 | 0.2 | 37 | 1.4 | 17 | 10 | 24 | 15 | 7 |
| | 650 | 550 | <0.15 | −100 | 3.5 | 18 | | | 35 | 47 |
| LHCII-control | 510 | 550 | 0.2 | −88 | 1.9 | 24 | 11 | 51 | 20 | 5 |
| | 510 | 680 | 0.2 | −50 | 2.3 | −29 | | | 50 | 50 |
| | 650 | 550 | <0.15 | −100 | 3.4 | 27 | | | 40 | 33 |

[a] Negative amplitudes correspond to rise components.

the lifetime of the carotenoid $S_1$ state. Interestingly, it is (within the experimental error) the same for all studied LHCII samples despite the fact that the $S_1$ lifetimes of Vio, Lut, and Zea are quite different in solution: 24 ps (Vio), 14 ps (Lut), and 9 ps (Zea) (*21*, *36*). The kinetics probed at the peaks of the carotenoid $S_1-S_N$ spectra with 650 nm excitation can be successfully fitted without the 11 ps decay component, confirming the assignment of this time constant to the $S_1$ lifetime of the carotenoids (see Table 1).

To study the spectral and dynamical properties of the $S_1$ state of all three carotenoids in the LHCII complex in more detail, the kinetics and transient spectra were measured in the near-infrared region, where ESA corresponding to the $S_1-S_2$ transition of carotenoids can be observed (*21*, *26*). These experiments were performed only on the LHCII samples reconstituted with a single carotenoid. Because of the more efficient $S_2-Q_x$ energy transfer in the LHCII-control complex, resulting in a low population of the $S_1$ state of carotenoids, the weak signals corresponding to the $S_1-S_2$ transition were beyond the detection limit of our experimental setup. The kinetics probed at 1600 nm shown in Figure 7 exhibit decay properties similar to those of the kinetics probed at the maxima of the $S_1-S_N$ transitions, indicating that a substantial part of the signal is indeed due to the $S_1-S_2$ transition (see Table 1). However, because the $S_1-S_2$ transition is significantly weaker than the $S_1-S_N$ transition, the relative ESA contributions originating from chlorophylls are substantially stronger in the near-infrared region. Also, a fast-decaying component of about 200 fs is observed in the 1600 nm kinetics. This component, which is not present in the kinetics measured at the maximum of the $S_1-S_N$ transition, was already observed in the IR region for other carotenoids and was attributed to the $S_2-S_N$ excited-state absorption (*21*, *26*).

To obtain information about the energy of the carotenoid $S_1$ state, transient absorption spectra in the near-infrared region corresponding to the $S_1-S_2$ transition are required. However, a direct measurement of the IR transient absorption spectra is hampered by contributions from chlorophyll ESA. Therefore, to obtain a "pure" spectral profile of the $S_1-S_2$ transition, the kinetics were measured in the wavelength region from 1200 to 1800 nm in steps of 10 nm. All the kinetics were then normalized to a signal value at 60 ps, because at this time most of the signal is due to the Chl-a ESA. From these normalized kinetics the transient absorption spectra were reconstructed. The transient spectra at a 6 ps time delay obtained by this normalization procedure are shown in Figure 8. Due to the normalization, these transient absorption spectra represent a spectral profile associated with the 11 ps decay of the carotenoid $S_1$ state, and thus display the carotenoid $S_1-S_2$ absorption spectrum. The normalized 6 ps spectra have distinct maxima at 6500 $cm^{-1}$ (1540 nm) for LHCII-Vio, 6100 $cm^{-1}$ (1640 nm) for LHCII-Lut, and 6200 $cm^{-1}$ (1610 nm) for the LHCII-Zea sample. For comparison, the transient spectra at a 60 ps time delay reconstructed from the kinetics *before* normalization and thus associated with the spectral profile of Chl-a are also shown. The maxima of the 60 ps spectra are shifted significantly to higher energies for all three samples.

Table 2: Amplitudes (%) of the Three Decay Components of Chl-a Fluorescence in the Reconstituted LHCII Complexes As Detected at 700 nm after 650 nm Excitation[a]

| | 0.5 ns | 1.5 ns | 3.5 ns | $\tau_{av}$ (ns) |
|---|---|---|---|---|
| LHCII-Zea | 26 | 53 | 21 | 1.1 |
| LHCIIVio | 16 | 33 | 51 | 1.5 |
| LHCII-Lut | 8 | 45 | 47 | 1.7 |
| LHCII-control | 2 | 36 | 62 | 2.2 |

[a] Averaged lifetimes $\tau_{av}$ were calculated as a sum of the rates weighted according to their amplitudes.

To explore fluorescence quenching in the LHCII complexes reconstituted with a single carotenoid, we measured the chlorophyll fluorescence of all studied complexes by means of time-correlated single-photon counting. All complexes were excited at the maximum of the Chl-b absorption (650 nm), and the Chl-a fluorescence was detected at 700 nm. The kinetics for the LHCII-control and LHCII-Zea complexes are shown in Figure 9, and fitting results for all studied complexes are summarized in Table 2. Three decay components with lifetimes of about 3.5, 1.5, and 0.5 ns were necessary to obtain satisfying fits. These three time components are present in all kinetics, but their amplitudes are markedly different. The shortest subnanosecond decay component is negligible in the LHCII-control sample having an amplitude of about 2%. The amplitude of this 0.5 ns component increases for the LHCII complexes reconstituted with a single carotenoid and reaches a maximum of 26% for the LHCII-Zea complex. Somewhat opposite behavior

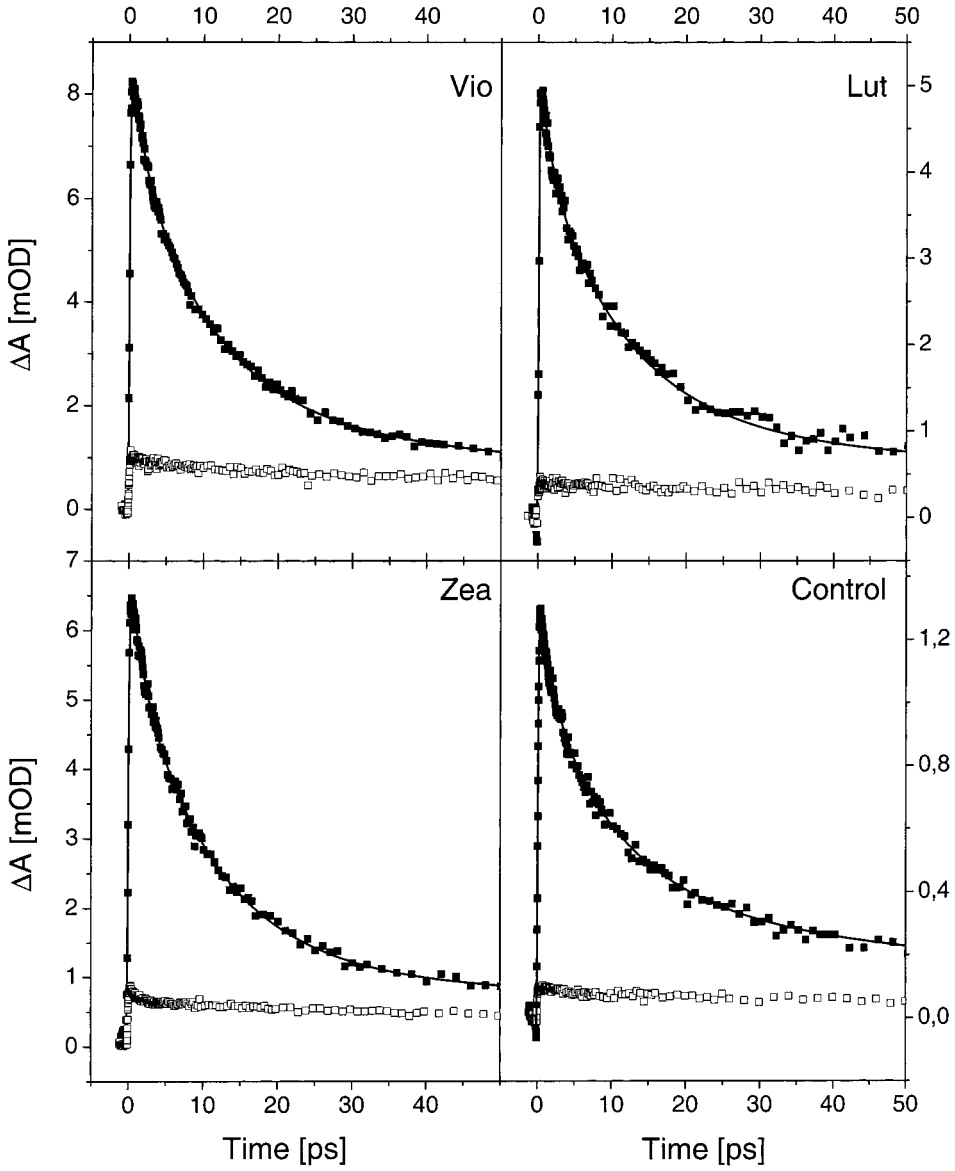


FIGURE 6: Kinetics recorded at the maxima of the carotenoid $S_1-S_N$ transitions in the LHCII complexes probed at 540 nm (LHCII-Vio), 550 nm (LHCII-Lut), 565 nm (LHCII-Zea), and 550 nm (LHCII-control) after excitation of carotenoids at 510 nm (full squares). Kinetics probed at the same wavelengths after excitation of Chl-b at 650 nm are also shown (open squares). The intensities of both 510 and 650 nm excitations were set to produce the same Chl-a bleaching signal at 680 nm.

is observed for the longest 3.5 ns component: it dominates the decay of the LHCII-control sample (62%), but is as low as 21% in the LHCII-Zea complex. Averaged fluorescence lifetimes listed also in Table 2 confirm the progressive shortening of the fluorescence lifetimes. This result agrees well with the recently measured fluorescence yields of these samples (*37*), which are proportional to the averaged fluorescence lifetimes observed here, suggesting that the decrease in fluorescence lifetimes is indeed due to an activation of energy-dissipating mechanisms with increased efficiency in the order control < Lut < Vio < Zea.

## DISCUSSION

The steady-state absorption spectra of the recombinant LHCII complexes (Figure 1) and the kinetics related to the Chl-b to Chl-a transfer (Figure 4) do not exhibit any dramatic changes when compared to those of the control sample. This clearly shows that the reconstitution of the LHCII complexes with a single carotenoid species does not affect their overall function as antennae. The presence of an ultrafast (<200 fs) rise component in the 680 nm kinetics after 510 nm excitation (Table 1) is a clear indication of the carotenoid $S_2$ to Chl $Q_x$ energy-transfer pathway. The slower rise of the Chl-a signal corresponds to energy transfer among chlorophyll species on the time scale of 0.2−6 ps. Such dynamics is characteristic of native LHCII complexes (*1*, *17*, *18*). The differences in the amplitudes of the kinetic components among reconstituted LHCII complexes can be attributed to differing Chl-a/Chl-b ratios. Despite the fact that the overall function is well conserved in the LHCII complexes containing a single carotenoid, the amplitudes of the carotenoid $S_1-S_N$ absorption shown in Figure 3b indicate a lower efficiency of the $S_2-Q_x$ energy-transfer pathway in these complexes. Such a decrease of efficiency can be connected with the lack of one Neo, since the selective binding site N1 is empty in all complexes considered here except for LHCII-control. Indeed, very recently (*18*) it was shown that Neo transfers energy predominantly from the $S_2$ state with a characteristic transfer

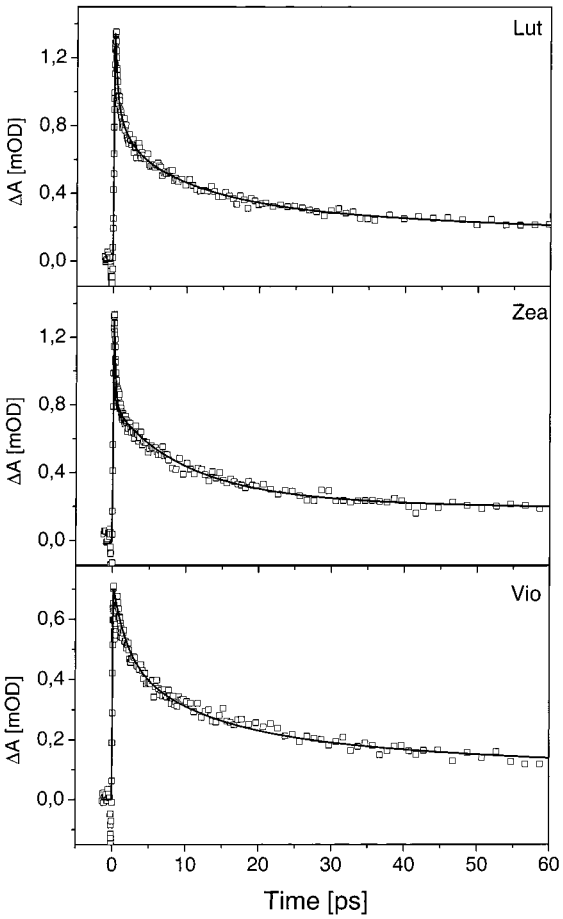


FIGURE 7: Kinetics of the LHCII complexes reconstituted with a single carotenoid corresponding to the $S_1-S_2$ transition detected at 1600 nm.

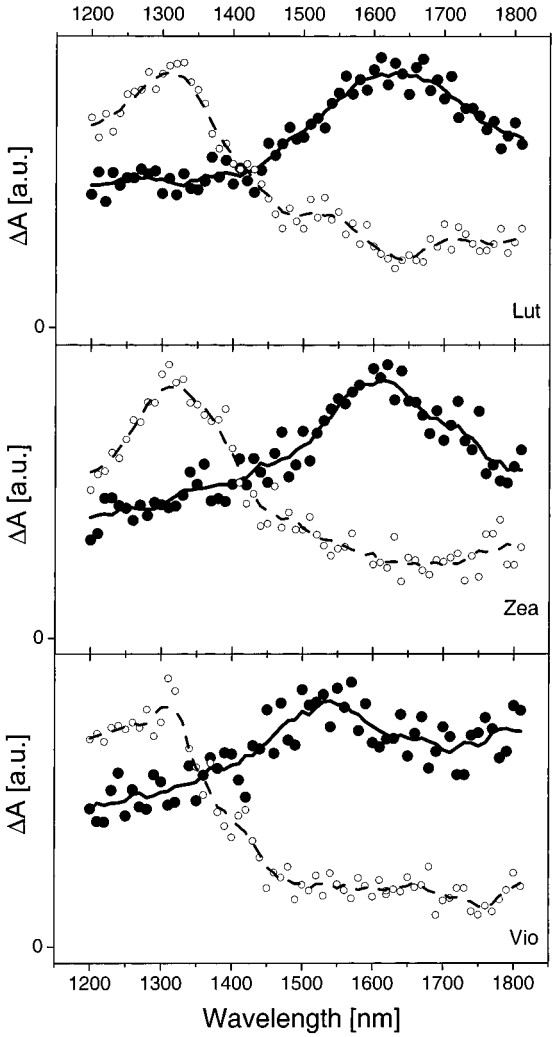


FIGURE 8: Normalized infrared transient absorption spectra of the reconstituted LHCII complexes detected at 6 ps and thus associated with the $S_1$ state of carotenoids (solid circles) and at 60 ps corresponding to the excited-state absorption of Chl-a (open circles). The solid (dashed) lines are results of Fourier transform smoothing of the raw data. All spectra are normalized to the maximum. See the text for details.

time of about 90 fs. Since Neo is absent in the LHCII reconstituted with Vio, Zea, or Lut, a decrease of the $S_2-Q_x$ transfer efficiency is necessarily expected in these complexes. Nevertheless, on the basis of the data shown here, we cannot unequivocally exclude a possibility that the empty carotenoid site in the LHCII complexes reconstituted with a single carotenoid can also somehow affect the overall $S_2-Q_x$ energy-transfer efficiency.

The primary goal of the present work was to determine the $S_1$ energy of carotenoids in the LHCII complex. On the basis of the transient absorption spectra associated with the decay of the $S_1$ level of all three carotenoids presented in Figure 8, together with the detailed analysis of the carotenoid region of the steady-state absorption spectra of all three studied samples, we can calculate the energies of the $S_1$ levels of all three carotenoids in their natural protein environment by subtracting the 0−0 energies associated with the $S_0-S_2$ and $S_1-S_2$ transitions (*21*, *26*). The energies of the $S_0-S_2$ transitions of Vio, Lut, and Zea in the reconstituted LHCII complex as extracted from the fits of the steady-state absorption spectra in the Soret region are 20200 ± 100 $cm^{-1}$ (Vio), 20150 ± 150 $cm^{-1}$ (Lut), and 20050 ± 100 $cm^{-1}$ (Zea). The $S_2$ energy of Lut was taken as the average energy of the two spectral forms corresponding to the L1 and L2 sites resolved in the fitting of the Soret absorption band (Figure 2). The spectral bands observed in the near-infrared transient absorption spectrum and associated with the 11 ps decay (Figure 7) give the following $S_1-S_2$ transition energies: 6500 ± 200 $cm^{-1}$ (LHCII-Vio), 6100 ± 150 $cm^{-1}$ (LHCII-Lut), and 6200 ± 100 $cm^{-1}$ (LHCII-Zea). A direct subtraction, $E(S_0-S_2) - E(S_1-S_2)$, yields $S_1$ energies of carotenoids of 13700 ± 300 $cm^{-1}$ (Vio), 14050 ± 300 $cm^{-1}$ (Lut), and 13850 ± 200 $cm^{-1}$ (Zea). It is important to point out that Vio has $S_1$ energy lower than Zea in LHCII and that the energy difference between $S_1$ energies of Vio and Zea in vivo is significantly smaller than the difference of ∼400 $cm^{-1}$ measured in vitro (*21*, *22*). The $S_2$ energies in the LHCII are also much closer than those in solution. In fact, given the experimental errors of the measurements and the fitting accuracy itself, the $S_1$ energies are the same for all three carotenoid species incorporated into the LHCII complex. However, it is worth noting that the slightly lower $S_1$ energy of Vio is consistent with the observed $S_1-S_N$ spectra, suggesting the strongest interaction and consequently the greatest red shift of the energy levels of Vio in the reconstituted LHCII complex.

It is necessary to point out that the assignment of the band located at around 1600 nm, observed in the transient spectra in Figure 8, to the 0−0 band of the $S_1-S_2$ transition is crucial

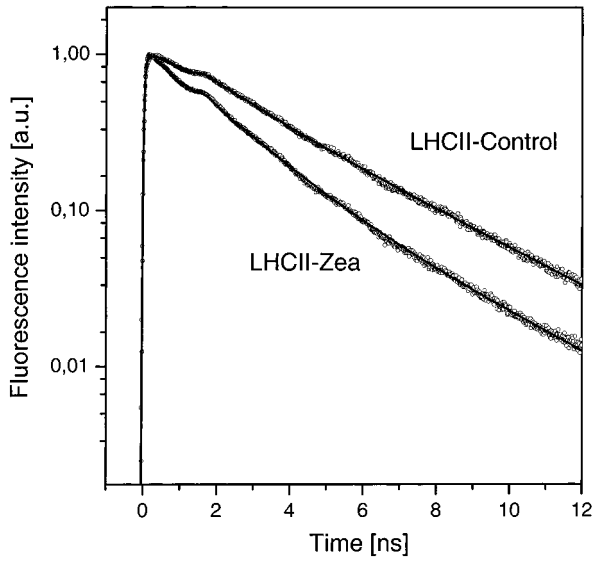


FIGURE 9: Kinetics and corresponding multiexponential fits of the Chl-a fluorescence of the LHCII-control and LHCII-Zea complexes detected at 700 nm after excitation of Chl-b at 650 nm.

to obtain the values of the $S_1$ energies given above. As discussed in ref 26 for the carotenoid spheroidene, if the observed band were due to the 0−1 vibrational transition, the real 0−0 band would be at lower energies and the calculated $S_1$ energies would actually be underestimated by one vibrational transition (∼1350 $cm^{-1}$). On the basis of the $S_1$ lifetimes and the corresponding $S_1$ energies of various carotenoids in solution, either experimentally measured (*38*) or estimated from the energy gap law (*15*), the calculated energies of about 13900 $cm^{-1}$ agree well with the observed lifetime of ∼11 ps. The spectral width of the observed bands further supports our assignment of the detected absorption bands to the lowest 0−0 electronic transition. The ESA bands in the 6 ps infrared transient spectrum of both LHCII-Vio and LHCII-Zea, shown in Figure 7, have a spectral width of about 900 $cm^{-1}$, which is similar to the width of the 0−0 bands of the $S_1-S_2$ transition of Vio and Zea in methanol (*21*). Since the $S_1-S_N$ transient absorption bands are a little wider in the LHCII complex than in solution (Figure 4), it is unlikely that the 0−1 band of the $S_1-S_2$ transition, which is broadened by the presence of two dominant vibrational modes (C−C and C═C stretches) (*39*), would have the same width as the 0−0 band in solution. This fact strongly supports our assignment of the 1600 nm band peak as the 0−0 vibrational band of the $S_1-S_2$ transition. In the LHCII-Lut sample this band is slightly broader (1050 $cm^{-1}$), most likely due to the overlap of two lutein transitions associated with L1 and L2 binding sites, again with good agreement with both steady-state absorption and the $S_1-S_N$ transient absorption spectra. Moreover, it has been shown that the $S_1$ level of short-chain carotenoids is shifted in the same direction as the $S_2$ state (*40*). Since in the reconstituted LHCII complexes the $S_2$ states of all three carotenoids are red-shifted with respect to methanol solution, also the $S_1$ levels are expected to be slightly red-shifted from those observed in solution. The $S_1$ levels of Vio and Zea in methanol determined by near-infrared time-resolved spectroscopy are 14470 ± 100 and 14030 ± 100 $cm^{-1}$ (*21*); therefore, the calculated energies of 13900 ± 300 $cm^{-1}$ in the LHCII complexes are in accord with this expectation. Thus, on the basis of the transient absorption spectra shown in Figure 8 and the measured lifetimes of the $S_1$ level of all three studied samples, we conclude that the $S_1$ energies of Vio, Lut, and Zea incorporated into the L1 and L2 sites of the LHCII antenna complex are, within experimental error, the same, having an energy of ∼13900 $cm^{-1}$. Keeping in mind that the lowest $Q_y$ transition of Chl-a in the LHCII complex is at about 14700 $cm^{-1}$, the carotenoid $S_0-S_1$ transition is low enough to enable a direct quenching of the chlorophyll $Q_y$ excited states via the $S_1$ state of carotenoids.

The transient absorption spectra in the visible region presented in Figure 3 are the key data to answer the question of whether fast back energy transfer on the picosecond time scale occurs from chlorophylls to the carotenoid $S_1$ state (direct quenching mechanism) in the LHCII complex. The characteristic signal corresponding to the $S_1-S_N$ transition of carotenoids was observed only when the carotenoids were excited directly. Tuning the excitation to 650 nm, and thus exciting only the Chl-b molecules, no distinct features appear at wavelengths lower than 630 nm. The kinetics measured at wavelengths corresponding to the maxima of the $S_1-S_N$ bands with both 510 and 650 nm excitation (Figure 6) support this conclusion: the 11 ps decay time is observed only when carotenoids are directly excited. All these observations lead to the conclusion that there is no fast direct $Q_y-S_1$ energy transfer occurring on the picosecond time scale in LHCII, the same being true for all reconstituted LHCII complexes independently on carotenoid species occupying the L1 and L2 sites. Also, a comparison between LHCII-control and the LHCII-Lut shows that the occupancy of the N1 site is also ineffective in this respect. Nevertheless, even though we cannot detect any direct Chl-a $Q_y$ to carotenoid $S_1$ quenching, it is not possible to rule out this channel yet. Because of the nanosecond Chl-a lifetime, excitations trapped at Chl-a can actually be transferred to the $S_1$ state of Zea on a time scale significantly longer than 100 ps. In such a case, given the Zea $S_1$ lifetime on the order of 10 ps, the population of the $S_1$ state would be extremely low and thus prevent detection of the $S_1$ excited-state absorption by conventional time-resolved spectroscopy methods even if a substantial fraction of the excitation energy were transferred through this channel.

The next question to answer is whether the carotenoid $S_1$ state can be an energy donor capable of providing an $S_1-Q_y$ energy-transfer pathway as an alternative to the efficient $S_2-Q_x$ pathway. Although locating the carotenoid $S_1$ energies below the $Q_y$ transition of chlorophylls seems to exclude this possibility, a few recent works revealed energy-transfer processes attributable to such an energy transfer (*17*−*19*). First of all, it is clear that the 11 ps process identified in the experiments presented here is due to the carotenoid $S_1-S_0$ internal conversion, since no corresponding rise of the Chl-a bleaching was observed. Nevertheless, the kinetics measured at the maxima of the $S_1-S_N$ transitions upon excitation at 510 nm (see Table 1 and Figure 4) contain, in addition to the main 11 ps decay, another decay component characterized by a time constant of about 1.9 ps. Somewhat longer decay components (15 and 3.9 ps) were recently observed by Croce et al. (*18*) and ascribed to the $S_1$ lifetimes of the two luteins in the LHCII complex. Because the 1.9 ps process occurs on a time scale similar to that of the Chl-b to Chl-a transfer, it is not easy to definitely assign the origin of this component.

A careful inspection of the amplitudes of the various kinetic components in Table 1 reveals that the amplitude of this time component observed in the $S_1-S_N$ kinetics excited at 510 nm is too high to be ascribed solely to the Chl-b to Chl-a transfer: the ESA signals from chlorophylls in this spectral region are at least 10 times weaker than those from carotenoids. Thus, we cannot rule out that the 1.9 ps component observed here is at least partially due to the transfer from carotenoid $S_1$ to $Q_y$ of Chl-a. In such a case a small fraction of excitation energy (~20% of the total $S_1$ population) can be transferred to the chlorophylls via the carotenoid $S_1$ state. However, since the $S_1$ energy was concluded to be below the $Q_y$ transition of chlorophylls, it is tempting to suggest that this energy-transfer pathway between carotenoids and chlorophylls somehow involves higher vibrational states of the carotenoid $S_1$ state. Indeed, the first excited vibrational level of the $S_1$ state would already be high enough to allow an energy transfer to chlorophylls, because the spacing between the vibrational levels of carotenoids (~1350 $cm^{-1}$) puts the 0−1 band of the $S_0-S_1$ transition at ~15250 $cm^{-1}$ (655 nm). This (or a higher) vibrational state could be a potential energy donor to the Chl-a $Q_y$ state. It is interesting to note that the energy of the carotenoid $S_1$ 0−1 vibrational band agrees within experimental error with the $S_1$ energy obtained from the two-photon excitation spectrum measured by Walla et al. (*19*). Since the two-photon absorption experiment relies on detection of upconverted Chl-a fluorescence, and thus on carotenoid $S_1$ to Chl-a energy transfer, the two-photon excitation spectrum is rather an action spectrum not necessarily related to the lowest 0−0 transition. This also supports the hypothesis that the first excited vibrational level of the carotenoid $S_1$ state could be involved in the $S_1-Q_y$ energy transfer. Very recently, this hypothesis was further confirmed by comparing the two-photon absorption spectra of the carotenoids in solution and in LHCII complexes (*41*).

Another intriguing feature of carotenoids in the reconstituted LHCII is their $S_1$ lifetime, exhibiting the same value of ~11 ps in all complexes. Having different conjugation lengths, the three investigated carotenoids in the LHCII complex are spectrally well distinguished in both steady-state and transient absorption spectra (Figures 2 and 3), but the kinetic properties of the $S_1$ state are, within the accuracy of the experiments, the same. This result is at first sight rather surprising, because the $S_1$ dynamics in solution of Vio, Lut, and Zea differ substantially; the corresponding lifetimes obtained in methanol are 24 ps (Vio), 14 ps (Lut), and 9 ps (Zea). This trend of the $S_1$ lifetimes can be rationalized via the energy gap law (*15*), as a result of the downshift of the $S_1$ energy by about 400 $cm^{-1}$ when the conjugation length increases from 9 (Vio) to 11 C═C bonds (Zea) (*21*, *22*). However, our results show that in LHCII all three carotenoids have approximately the same energy, strongly suggesting that the $S_1$ lifetimes should also be the same, as is in fact observed. The change of the $S_1$ lifetime in going from solution to protein is most pronounced for LHCII-Vio, while LHCII-Zea remains almost unaffected, again in good agreement with the observed energies: ~13900 $cm^{-1}$ for LHCII-Zea is close to the $S_1$ energy of Zea in solution (*21*, *22*). These results also suggest that stronger carotenoid−protein interactions occur when violaxanthin is incorporated into the LHCII structure. This is supported by the $S_1-S_N$ spectra shown in Figure 4, where the shift between the transient spectra in solution and in the protein is largest for the LHCII-Vio complex. All these observations reveal that the LHCII protein structure significantly affects the properties of the $S_1$ state of carotenoids, and this effect is strongest in the case of Vio.

Using femtosecond transient absorption measurements over a broad spectral range and a time window extending up to 100 ps, we have shown that the direct quenching of chlorophyll excited states by the carotenoid $S_1$ state cannot be detected on this time scale. However, the measurements of Chl-a fluorescence lifetimes on the nanosecond time scale revealed clear differences between the studied LHCII complexes; while no subnanosecond component was necessary to fit the fluorescence decay of the LHCII-control complex, incorporation of Zea into the LHCII complex leads to a quenching of the Chl-a fluorescence characterized by a 0.5 ns decay component (Table 2 and Figure 9). A similar behavior was recently found in other recombinant proteins from the Lhc family reconstituted with a single carotenoid, CP26 (*25*) and CP29 (*24*). Thus, although there is no observable direct energy transfer on the picosecond time scale from the chlorophyll $Q_y$ state to the carotenoid $S_1$ state in LHCII-Zea, the occurrence of Zea in LHCII and related complexes promotes the quenching of chlorophyll fluorescence. The binding of Lut, Vio, and Zea to the LHCII complex modulates the photochemical characteristics of these xanthophylls, making their $S_1$ energies and lifetimes virtually the same, although they are clearly different in an organic solvent. It is thus unlikely that the observed fluorescence quenching relies on the photochemical properties of the carotenoid species themselves. This observation strongly supports a quenching mechanism proposed very recently by some of us (*24*, *42*). According to this proposal, carotenoids induce quenching by modifying the Lhcb protein folding through their binding to the L2 site, which thus appears to be an allosteric site able to trigger a quenching of the Chl-a excited states. The presence of at least two different conformations of Lhcb proteins was recently demonstrated by spectroscopic methods (*43*). The data presented here support this idea, and also indicate that the quencher can be either the Chl-a itself or a carotenoid $S_1$ state that directly quenches Chl-a, but on a slower time scale (~0.5 ns). The hypothesis of Chl-a molecules as quenchers was already suggested some time ago (*44*, *45*) and involves formation of Chl-a excitonic pairs as a result of conformational changes. However, such a formation of excitonic pairs coupled sufficiently to produce a significant quenching of the chlorophyll excited states should be demonstrated by changes in both absorption and fluorescence spectra, because the splitting of the chlorophyll states caused by the excitonic interaction would shift the chlorophyll $Q_y$ states toward lower energy. Despite the fact that we did not observe any significant changes in the absorption spectra, the fluorescence spectra of the reconstituted LHCII complexes published recently (*3*) revealed a small red shift of the fluorescence spectrum of the LHCII-Zea sample. Although this observation could be interpreted as due to formation of a Chl-a excitonic pair, together with no observable changes in the absorption spectrum, the effect seems to be too small to account for the efficient fluorescence quenching observed in the LHCII-Zea complex. On the other hand, a slow sub-

nanosecond transfer of energy from Chl-a to the $S_1$ state of Zea could actually provide an efficient quenching channel, because the 11 ps $S_1$ lifetime of Zea in the LHCII complex would play the role of an effective sink for excitations transferred from Chl-a. Thus, although the experimental data cannot unambiguously assign the exact mechanism of the observed fluorescence quenching, energy transfer from the $Q_y$ state of Chl-a to the $S_1$ state of Zea occurring on the ~0.5 ns time scale seems to be a promising candidate to explain the fluorescence quenching. However, contrary to the previous suggestions (*20*), the key presence of Zea is not due to intrinsic photophysical properties of this carotenoid, but rather due to its ability to promote a conformational change allowing such a transfer, even though on a time scale about 3 orders of magnitude slower than the conventional energy transfer within the LHCII complex.

## ACKNOWLEDGMENT

We thank Arvydas Ruseckas for his help with the single-photon-counting measurements, Hans-Erik Åkerlund for providing us purified violaxanthin and zeaxanthin, Roberta Croce for discussions and help with the deconvolution of the steady-state absorption spectra, and Jennifer Herek and Tõnu Pullerits for valuable discussions.

## REFERENCES

1. van Amerongen, H., and van Grondelle, R. (2001) *J. Phys. Chem. B 105*, 604−617.
2. Sieferman, H. (1987) *Physiol. Plant. 69*, 561−568.
3. Croce, R., Weiss, S., and Bassi, R. (1999) *J. Biol. Chem. 274*, 29613−29623.
4. Demmig-Adams, B. (1990) *Biochim. Biophys. Acta 1020*, 1−24.
5. Kühlbrandt, W., Wang, D. N., and Fujiyoshi, Y. (1994). *Nature 367*, 614−621.
6. Dainese, P., and Bassi, R. (1991) *J. Biol. Chem. 266*, 8136−8142.
7. Bassi, R., Pineau, B., Dainese, P., and Marquardt, J. (1993) *Eur. J. Biochem. 212*, 297−303.
8. Ruban, A. V., Lee, P. J., Wentworth, M., Young, A. J., and Horton, P. (1999) *J. Biol. Chem. 274*, 10458−10456.
9. Verhoeven, A. S., Adams, W. W., III, Demmig-Adams, B., Croce, R., and Bassi, R. (1999) *Plant Physiol. 120*, 1−11.
10. Gradinaru, C. C., Pascal, A. A., van Mourik, F., Robert, B., Horton, P., van Grondelle, R., and van Amerongen, H. (1998) *Biochemistry 37*, 1143−1149.
11. Agarwal, R., Krueger, B. P., Scholes, G. D., Yang, M., Yom, J., Mets, L., and Fleming, G. (2000) *J. Phys. Chem. B 104*, 2908−2918.
12. Connelly, J. P., Müller, M. G., Hucke, M., Gatzen, G., Mullineaux, C. W., Ruban, A. V., Horton, P., and Holzwarth, A. R. (1997) *J. Phys. Chem. B 101*, 1902−1909.
13. Christensen, R. (1999) in *Photochemistry of Carotenoids* (Frank, H. A., Young, A. J., Britton, G., and Cogdell, R. J., Eds.) pp 137−159, Dordrecht, The Netherlands.
14. Macpherson, A., and Gillbro, T. (1998) *J. Phys. Chem A 102*, 5049−5058.
15. Chynwat, V., and Frank, H. A. (1995) *Chem. Phys. 194*, 237−244.
16. Connelly, J. P., Müller, M. G., Bassi, R., Croce, R., and Holzwarth, A. R. (1997) *Biochemistry 36*, 281−287.
17. Gradinaru, C. C., van Stokkum, I. H. M., Pascal, A. A., van Grondelle, R., and van Amerongen, H. (2000) *J. Phys. Chem. 104*, 9330−9342.
18. Croce, R., Müller, M. G., Bassi, R., and Holzwarth, A. R. (2001) *Biophys. J. 80*, 901−915.
19. Walla, P. J., Yom, J., Krueger, B. P., and Fleming, G. (2000) *J. Phys. Chem. B 104*, 4799−4806.
20. Frank, H. A., Cua, A., Chynwat, V., Young, A., Gosztola, D., and Wasielewski, M. R. (1994) *Photosynth. Res. 41*, 389−395.
21. Polívka, T., Herek, J. L., Zigmantas, D., Åkerlund, H.-E., and Sundström, V. (1999) *Proc. Natl. Acad. Sci. U.S.A. 96*, 4914−4917.
22. Frank, H. A., Bautista, J. A., Josue, J. S., and Young, A. J. (2000) *Biochemistry 39*, 2831−2837.
23. Richter, M., Goss, R., Wagner, B., and Holzwarth, A. R. (1999) *Biochemistry 38*, 12718−12726.
24. Crimi, M., Dorra, D., Bösinger, C. S., Giuffra, E., Holzwarth, A. R., and Bassi, R. (2001) *FEBS Lett. 268*, 260−267.
25. Frank, H. A., Das, S. K., Bautista, J. A., Bruce, D., Vasilev, S., Crimi, M., Croce, R., and Bassi, R. (2001) *Biochemistry 40*, 1220−1225.
26. Polívka, T., Zigmantas, D., Frank, H. A., Bautista, J. A., Herek, J. L., Koyama, Y., Fujii, R., and Sundström, V. (2001) *J. Phys. Chem. B 105*, 1072−1080.
27. Fujii, R., Onaka, K., Kuki, M., Koyama, Y., and Watanabe, Y. (1998) *Chem. Phys. Lett. 288*, 847−853.
28. Sashima, T., Shiba, M., Hashimota, H., Nagae, H., and Koyama, Y. (1998) *Chem. Phys. Lett. 290*, 36−42.
29. Matsouka, M., Kano-Murakami, Y., and Yamamoto, N. (1987) *Nucleic Acids Res. 15*, 6302.
30. Bujard, H., Gentz, R., Lanzer, M., Stüber, D., Müller, M., Ibrahimi, I., Hauptle, M. T., and Dobberstein, B. (1987) *Methods Enzymol. 155*, 416−433.
31. Giuffra, E., Cugini, D., Croce, R., and Bassi, R. (1996) *Eur. J. Biochem. 238*, 112−120.
32. Gilmore, A. M., and Yamamoto, H. Y. (1991) *J. Chromatogr. 543*, 137−145.
33. Croce, R., Cinque, G., Holzwarth, A., and Bassi, R. (2000) *Photosynth. Res. 64*, 221−231.
34. Cinque, R., Croce, R., and Bassi, R. (2000) *Photosynth. Res. 64*, 233−242.
35. Frank, H. A., Bautista, J. A., Josue, J., Pendon, Z., Hiller, R. G., Sharples, F. P., Gosztola, D., and Wasielewski, M. R. (2000) *J. Phys. Chem. B104*, 4569−4577.
36. Frank, H. A., Chynwat, V., Desamero, R. Z. B., Farhoosh, R., Erickson, J., and Bautista, J. A. (1997) *Pure Appl. Chem. 69*, 2117−2124.
37. Formaggio, E., Cinque, G., and Bassi, R. (2001) *J. Mol. Biol. 314*, 1157−1166.
38. Frank, H. A., Desamero, R. Z. B., Chynwat, V., Gebhard, R., van der Hoef, I., Jansen, F. J., Lugtenburg, J. Gosztola, D., and Wasielewski, M. R. (1997) *J. Phys. Chem. A 101*, 149−157.
39. Christensen, R. L., Goyette, M., Gallagher, L., Duncan, J., DeCoster, B., Lugtenburg, J., Jansen, F. J., and van der Hoef, I. (1999) *J. Phys. Chem. A 103*, 2399−2407.
40. Andersson, P.-O., Bachilo, S. M., Chen, R.-L., and Gillbro, T. (1995) *J. Phys. Chem. 99*, 16199−16209.
41. Walla, P., Linden, P. A., Ohta, K., and Fleming, G. R. (2001) *J. Phys. Chem. A*, in press.
42. Bassi, R., and Caffari, S. (2000) *Photosynth. Res. 64*, 243−256.
43. Moya, I., Silvestri, M., Cinque, G., and Bassi, R. (2001) *Biochemistry 40*, 12552−12561.
44. Crofts, A. R., and Yerkes, C. T. (1994) *FEBS Lett. 352*, 265−270.
45. Horton, P., Ruban, A. V., and Walters, R. G. (1996) *Annu. Rev. Plant Physiol. Plant Mol. Biol. 47*, 655−684.

BI011589X